Macrocyclization Equilibria. 2. Poly(dimethylsiloxane)

U. W. Suter, M. Mutter, and P. J. Flory*

Contribution from the Department of Chemistry, Stanford University, Stanford, California 94305. *Received March 3, 1976*

Abstract: Cyclization equilibrium constants K_x for the formation of cyclic siloxanes $\overline{\text{-Si(CH}_3)_2\text{-O-}}_x$ from the linear polymer are examined on the basis of the theory presented in the preceding paper with particular attention to the range $7 \leq x \leq 30$. The configurational averages of the required moments and polynomials are calculated using exact matrix generation methods and Monte Carlo techniques. The density $W(\mathbf{0})$ of chain vectors at $\mathbf{r} = \mathbf{0}$ is considerably overestimated by the Gaussian approximation. Values of $W(\mathbf{0})$ calculated in higher approximation yield lower values of K_x, which are in satisfactory agreement with experiment for $x > 15$. For $7 \leq x \leq 15$, the discrepancies between theory and experiment are reduced but not eliminated by use of the more accurate values of $W(\mathbf{0})$. Further improvement is achieved by taking account of the orientational correlation between terminal bonds of the x-meric acyclic sequence, which is found by calculation to be unfavorable to cyclization for $x \geq 10$. At $x = 12$, the orientational correlation factor reduces K_x by about half, according to the computations. The factor increases toward unity with increase in x; at $x = 30$ a reduction of K_x of only about 10% is indicated. Although the calculations are unreliable for $x < 10$, an increase in the orientational correlation factor is intimated for $x < 6$, in harmony with the larger values of K_x observed for small rings. The calculations are in approximate agreement with the experimental results that have been reported for the cyclic siloxanes in the intermediate range of x but fail to reproduce detailed features of the observed dependence of K_x on x in the range $x = 10$–16.

Polymerization of disubstituted siloxanes invariably yields substantial quantities of cyclic products

$$\overline{\text{-SiR}_2\text{-O-}}_x$$

at equilibrium.[1] The presence of an appreciable fraction of such material in poly(dimethylsiloxane) (PDMS), in which R = CH_3, was first observed by Scott.[2] Subsequently, a wealth of experimental data has been reported[3-6] on the concentrations of various cyclic oligomers of PDMS at equilibrium over the range $x = 3$ to 200. These concentrations, determined by chromatographic methods, equate to the cyclization equilibrium constant K_x defined in the preceding paper,[7] hereafter designated 1.

Results for $x > 20$ (i.e., for $n > 40$ bonds) determined in bulk and in poor solvents (near the theta point) have been shown to be approximately in agreement[1,7-10] with cyclization constants K_x calculated from eq 1-12 (spherical Gaussian density; directional correlations neglected), this being a variant of the relation (see eq 1-13) deduced by Jacobson and Stockmayer.[11] The parameter $\langle r_n^2 \rangle$ appearing in eq 1-12 was evaluated on the basis of experimental determinations of $\langle r^2 \rangle$ for linear PDMS of high molecular weight.[12] Conversion to values of $\langle r_n^2 \rangle$ for short chains was carried out according to rotational isomeric state theory.[13] Over the range $35 < x < 200$ experimental values of K_x for the equilibrated melt at 110 °C are only about 15% below those calculated in the foregoing manner.[1,6] Dilution with diglyme (a theta solvent) to a concentration of 220 g $l.^{-1}$ yielded[6] uniformly lower values of K_x throughout this range; departures from the calculations average about 25%. Although the discrepancies exceed the stated experimental errors severalfold, the measure of agreement is remarkably good in view of the fact that it is achieved without manipulation of adjustable parameters. (When the system is diluted with toluene, a good solvent, somewhat lower values of K_x are obtained for $x > 50$, apparently due to effects of excluded volume.[3,6])

As the size x of the ring is diminished, experimental values of K_x fail to increase as rapidly as predicted by eq I-12; see Figure 2 below. At $x = 16$ the discrepancy increases to ca. 30%,[5,6] i.e., the ratio of K_x(obsd) to K_x(calcd) according to eq 1-12 is ca. 0.70. At $x = 10$–11, this ratio falls to ca. 0.25. The observed equilibrium constant passes through a minimum at $x = 12$, the presence of which is attested by several separate investigations.[3-6] As x decreases further, K_x increases rapidly; for $x = 4$ and 5 it exceeds the values calculated according to eq 1-12 by a factor of 2–3.

At the outset of the present investigation, it appeared that the marked deviations in the range $7 \leq x \leq 16$ from the Jacobson–Stockmayer theory as expressed in slightly modified form by eq 1-12 might conceivably find explanation in (i) departures from the assumed spherical Gaussian distribution $W(\mathbf{0})$ about the zeroth atom of the chain and (ii) the effects of directional correlations discussed in 1 and embodied in the factor $2\Gamma_0(1)$; see eq 1-14.[7]

Calculations of moments by Chang[16,17] on PDMS chains of finite length point to severe deviations from the spherical Gaussian distribution for $x < 40$. In particular, the asymmetry of $W(\mathbf{r})$ reduces the density $W(\mathbf{0})$ appreciably at $\mathbf{r} = \mathbf{0}$. Hence, factor (i) was implicated as responsible, in part at least, for the departures of K_x from the Jacobson–Stockmayer theory in the intermediate range of x.

Beevers and Semlyen[8] had shown previously that approximate agreement with theory may be achieved for $x = 8$ and 9 by enumeration of all conformations and estimating the density $W(\mathbf{0})$ at $\mathbf{r} = 0$ from the sum of statistical weights for those conformations for which $|\mathbf{r}|$ falls within a specified small range about $\mathbf{r} = \mathbf{0}$. These computations suggested that factor (i), i.e., the non-Gaussian character of the distribution, may alone account for departures from the simpler theory for $x = 8$ and 9. The direct enumeration procedure of Beevers and Semlyen becomes inoperable for large x owing to the excessive number of conformations.

In this paper we report numerical calculations carried out with the object of examining the respective effects of (i) and (ii) above on values of the cyclization constants K_x for PDMS sequences in the range $7 \leq x \leq 30$.

Basis of the Computations

The PDMS chain in a conformation approaching the requirements for cyclization is illustrated in Figure 1 (compare Figure 1-1). The coordinate system of reference is defined by the bond pair Si–O and O–Si, the X axis being along the former bond. The choice of Si rather than O as the initial atom is arbitrary. Obviously, the chain comprising the sequence of $n = 2x$ atoms is the same regardless of which terminus, Si or O, is chosen as zeroth atom, or, equivalently, regardless of which bond, O–Si or Si–O, is established in forming the ring with n skeletal atoms. Thus, the value deduced for K_x must be

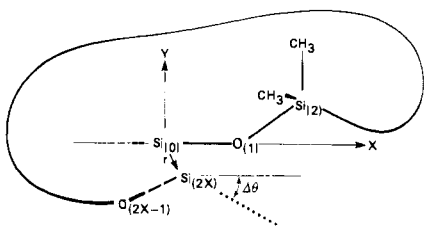

Figure 1. PDMS chain in a conformation with small end-to-end vector $\mathbf{r}_{2x}$ in the reference frame of the first Si-O bond. The angle $\Delta\theta$ gives the orientation of the hypothetical $(2x + 1)$th bond with respect to bond 1, i.e., the X axis.

the same in the respective reference frames affixed to Si-O-Si and O-Si-O. Moreover, the densities $W(\mathbf{0})$ of chain vectors at $\mathbf{r} = \mathbf{0}$ must be equal in the two representations for a chain each of whose units consists of two equivalent bonds, and hence has twofold symmetry. It follows from eq 1-10 that values of $2\Gamma_0(1)\bar{\Phi}$ must also be invariant to the choice of initial atom and frame of reference. Values of $2\Gamma_0(1)$ may differ only to the extent that $\bar{\Phi}$ differs in the two representations. We replace $\bar{\Phi}$ by unity in this work (see 1); differences in $2\Gamma_0(1)$ are presumed to be negligible.

The bond length l and bond angles were assigned the values $l = 1.64$ Å, $\angle SiOSi = 143°$, and $\angle OSiO = 110°$, the same having been used in previous investigations dealing with PDMS chains.[13,18] Rotational isomeric states were chosen at $\varphi = 0°$, $\pm 120°$ as before. Statistical weight matrices of the conventional form[13,18]

$$\mathbf{U} = \begin{bmatrix} 1 & \sigma & \sigma \\ 1 & \sigma & \sigma\omega \\ 1 & \sigma\omega & \sigma \end{bmatrix} \qquad (1)$$

with the three states indexed in the order t, g^+, and g^- were employed. In the matrix $\mathbf{U}_a$ for the bond Si-O preceded by O-Si, $\omega = \omega_a = 0$; in $\mathbf{U}_b$ for bond O-Si preceded by Si-O, $\omega = \omega_b$. The statistical weights were assigned values for a temperature of 110 °C as follows:[13] $\sigma = 0.327$ and $\omega_b = 0.25$.

The Probability Density $W(\mathbf{0})$ and Its Influence on K_x

The density $W(\mathbf{0})$ of chain vectors with $\mathbf{r} = \mathbf{0}$ is required for the calculation of $\langle P_k \rangle_{r=0}$ (see eq 1-22 and 1-27) as well as for the calculation of K_x. Its evaluation is difficult for short chains where the error of the Gaussian approximation is large[14,15] and series expansions in higher moments converge slowly.[10,15,16] In order to determine the most suitable approach for estimating $W(\mathbf{0})$, values obtained by different methods are compared. Instead of displaying $W(\mathbf{0})$, we plot the values of K_x calculated according to eq 1-11 with $\sigma_{cx} = 2x$, the relative orientation of the terminal bonds being ignored in this expression. The influence of the density distribution on K_x can thus be examined apart from the effects of other factors.

The density in the vicinity of $\mathbf{r} = \mathbf{0}$ was first calculated by generating Monte Carlo chains using conditional probabilities[15] obtained from the statistical weights given above, the number of chain termini falling within a sphere of radius δr about the origin being divided by the volume of the sphere. In order to achieve equitable sampling at each chain length, we let δr be proportional to $\langle r^2 \rangle^{1/2}$, taking $\delta r = 0.3 \langle r^2 \rangle^{1/2}$ or $\delta r = 0.5 \langle r^2 \rangle^{1/2}$. These domains sample about 4 and 11%, respectively, of the total populations. Calculations were carried out for chains having lengths $6 \leq x \leq 30$, with 30 000 chains being generated at each x. The densities deduced using the two domains are in good agreement. The larger sample with $\delta r = 0.5 \langle r^2 \rangle^{1/2}$ was subject to smaller statistical error and hence was used in subsequent calculations. The densities $W(\mathbf{0})$ thus

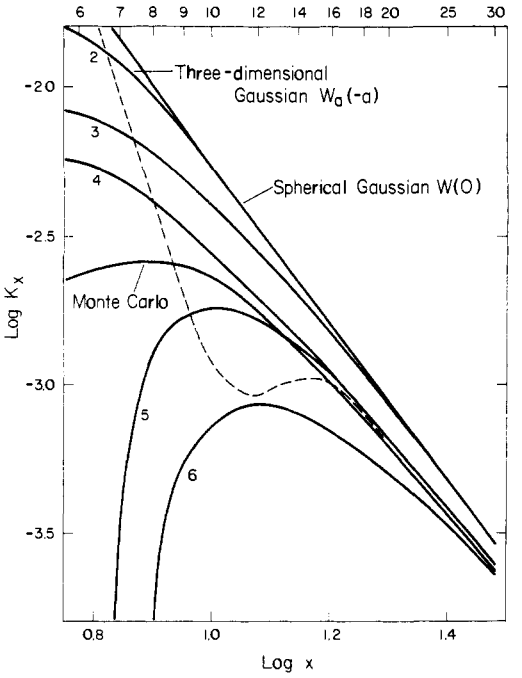

Figure 2. Cyclization equilibrium constants K_x calculated neglecting orientational correlations between chain ends. The various solid curves were calculated using the several approximations for $W(\mathbf{0})$ described in the text. The dashed curve summarizes experimental results; see Figure 6.

obtained for $7 \leq x \leq 9$ agree approximately with the results of Beevers and Semlyen[8] obtained by direct enumeration. Equilibrium constants K_x calculated from these densities according to eq 1-11, in which the directional factor $\Gamma_0(1)$ is ignored, are represented by the curve labeled "Monte Carlo" in Figure 2.

The curve labeled "spherical Gaussian" refers to the Gaussian distribution centered at $\mathbf{r} = \mathbf{0}$. It was obtained according to eq 1-12 from the second moment $\langle r_n^2 \rangle$ evaluated by standard methods.[19]

Curve 2 in Figure 2 was obtained by use of nonspherical Gaussian density[14,15] $W_a(\rho)$ centered at $\mathbf{r} = \mathbf{a}$ (see eq 1-29), where $\mathbf{a}$ is the persistence vector defined by $\mathbf{a} \equiv \langle \mathbf{r} \rangle$ and $\rho \equiv \mathbf{r} - \mathbf{a}$. Thus, $W(\mathbf{0})$ in eq 1-11 was equated to $W_a(-\mathbf{a})$. The distribution $W_a(\rho)$ is the product of three orthogonal Gaussians with moduli given by the eigenvalues of the second moment tensor $\langle \rho\rho^T \rangle$.

The other solid curves in Figure 2 were calculated by Chang[17] from the three-dimensional Hermite expansion[20] of $W_a(\rho)$ truncated at the tensor polynomial of the rank indicated for each curve. Relationships and procedures used are given elsewhere.[15,16,20] The decrease of K_x in Figure 2 with extension of the three-dimensional Hermite series up to terms of sixth rank reflects a corresponding trend in the values of $W(\mathbf{0}) = W_a(-\mathbf{a})$. It finds precedent in calculations of densities at $\mathbf{r} = \mathbf{0}$ for polymethylene chains with $n < 50$ bonds.[15] Presumably these trends would be reversed if higher terms were available to be included. Eventual convergence to the Monte Carlo curve in Figure 2 should be expected. Many additional terms evidently would be required however to realize this convergence.

The moment expansion truncated at the fourth tensor polynomial (involving moment tensors up to fourth rank) gives values of $W(\mathbf{0})$, and hence of K_x, in closer agreement with the results of the Monte Carlo calculations than expansions truncated at the fifth and sixth tensor polynomials. In fact, agreement of the fourth tensor polynomial calculations with the Monte Carlo results is quite satisfactory, for the purpose at hand, for $x > 8$.

Similar calculations were carried out using the ordinary Hermite series, cited in 1 (see eq 1-25 and 1-26), that involves the scalar even moments $\langle r^2 \rangle$, $\langle r^4 \rangle$, etc., the series being truncated at various Hermite polynomials up to g_{10}. The moments were evaluated by (exact) matrix generation.[19] Divergences of the K_x thus calculated from the results of the Monte Carlo calculations are generally greater than for the three-dimensional expansion. Truncation at g_4 yields a curve that is very close to curve "4" in Figure 2 for $x > 8$, and hence that approximates the "Monte Carlo" curve equally well. No explanations are apparent for this correspondence. However, it holds also for the systems treated in the following paper.[21] Accepted as an empirical observation, it facilitates subsequent calculations of $W(\mathbf{0})$ for $x > 8$, which are carried out using the ordinary Hermite expansion (eq 1-25) truncated at g_4. The moments $\langle r^2 \rangle$ and $\langle r^4 \rangle$ suffice, and these are readily computed.[19]

The dashed curve in Figure 2 joins mean values taken from experimental data.[3-6] These data are presented in full in Figure 6. Refinement of $W(\mathbf{0})$ beyond the usual Gaussian approximation in the manner indicated above brings theory and experiment into satisfactory agreement for $x > 15$. At $x = 16$, the Gaussian density $W(\mathbf{0})$ is about 40–45% greater than the more accurate estimates obtained by series expansion to the fourth moment or by Monte Carlo calculations, as reflected in the K_x values traced by the indicated curves in Figure 2. Convergence to the Gaussian density with increase in x is slow: at $x = 30$, the difference is ca. 20%; according to calculations beyond the range covered in Figure 2, a difference of ca. 10% persists at $x = 70$. For $x > 15$, the departures of $W(\mathbf{0})$ from Gaussian aappear to suffice to establish agreement between theory and experiment within probable limits of error.

The observed data for lower values of x, in the range $7 \leq x \leq 15$, exhibit large departures from values calculated according to 1-11 from either the "Monte Carlo" or the "fourth moment" densities $W(\mathbf{0})$. At $x = 11$ the discrepancy is most striking, K_x being only about half the value calculated according to eq 1-11 from the improved density $W(\mathbf{0})$.

At still smaller values of x, i.e., for $x < 7$, the cyclization constant rises above the "spherical Gaussian" curve. These high values of K_x appear to reflect favorable angle correlations, as was pointed out previously.[9,10] The statistical methods here employed fail for these shorter chains. Hence, comparison with calculations in this range is necessarily qualitative.

Directional Correlation Factors

Calculations of $\Gamma_0(1)$ according to eq 1-19 require averages $\langle P_k \rangle_{r=0}$ of the Legendre polynomials P_k, with $k = 0, 1, 2, \ldots$ and arguments $\gamma = \cos \Delta\theta$, over all configurations for which $\mathbf{r} = \mathbf{0}$. According to eq 1-22 (or 1-27) and 1-23, the averages $\langle P_k \rangle_{r=0}$ can be evaluated from moments $\langle P_k r^{2p} \rangle$ of the polynomials averaged without restriction on r. For small values of $k + p$, these in turn are conveniently evaluated from moments $\langle \gamma^m r^{2p} \rangle$ with $m \leq k$ (see 1), which can be calculated exactly by matrix multiplication methods[19] given in the Appendix to this paper. For larger $k + p$ the sizes of the matrices required become prohibitively large.

Alternatively, $\langle P_k \rangle_{r=0}$ may be estimated according to eq 1-22,23 by the Monte Carlo methods outlined in 1. Since the exact value of $\langle r^2 \rangle$ is easily computed by matrix methods,[10,19] it may be substituted in eq 1-23 at the outset, leaving $f_{k;2s}$ to be evaluated by taking the Monte Carlo average of the resulting polynomial as a whole. Analogously, the bracketed series occurring in eq 1-22 and in eq 1-27, truncated at the chosen 2s, can be averaged in its entirety after introducing the separately determined value of $\langle r^2 \rangle$ into each term.

In Figure 3 we show $\langle P_1 \rangle_{r=0} \equiv \langle \gamma \rangle_{r=0}$ calculated according to eq 1-27 truncated at terms of the indicated ranks $2s$, i.e., at $f_{1;2s}$, and plotted against x. All calculations were carried out using values of $\mathcal{H}(0)$ obtained from eq 1-25 truncated at g_4. Solid curves show results obtained from exact matrix multiplication calculations of the moments $\langle \gamma r^{2p} \rangle$, where $p = s, s - 1$, etc., with $2s = 0$, 2, and 4, respectively. The points and dashed curves represent Monte Carlo calculations of the averages $\langle P_1 \rangle_{r=0}$ evaluated in the manner stated above. Sets of 25 000 Monte Carlo chains, generated using conditional probabilities as above (see also 1), were employed for each chain length x. The error bars represent twice the standard deviation σ_m of the mean (*i.e.*, $2\sigma_m = 2\sigma N^{1/2}$ where N is the size of the Monte Carlo sample); they embrace confidence limits of ca. 95%. Differences between the Monte Carlo results for $2p = 4$ and the exact calculations (solid line 4) are well within the indicated error limits for all chain lengths x.

The first term $f_{1;0}$ required by the series in eq 1-27 for $\langle P_1 \rangle_{r=0}$ is positive for all x and converges rapidly to zero with increasing x; see Figure 3. The addition of $f_{1;2}$ makes $\langle P_1 \rangle_{r=0}$ negative for all $x > 4$. Inclusion of the next term, $f_{1;4}$, decreases $\langle P_1 \rangle_{r=0}$ further. However, curve 4 converges toward curve 2 with increase in x. At $x = 50$, where $\langle P_1 \rangle_{r=0}$ is -1.8×10^{-2}, only 18% of this value is due to $f_{1;4}$, the rest is due to $f_{1;2}$. Inclusion of $f_{1;6}$ in the series lowers the result substantially for $x < 10$. For higher x, however, $f_{1;6}$ tends toward zero, as is apparent from the fact that the curves representing $\langle P_1 \rangle_{r=0}$ calculated with eq 1-27 truncated at $f_{1;4}$ and $f_{1;6}$ differ imperceptibly for $x > 10$. The term $f_{1;8}$ becomes insignificant beyond $x = 5$. Thus, for $x > 10$, the result calculated by use of terms evaluated by exact matrix methods up to $f_{1;4}$ is adequate, while for $6 \leq x \leq 10$ the Monte Carlo results, including $f_{1;6}$, are to be preferred.

As a test of the foregoing procedure, 5000 Monte Carlo chains were generated for each chain length x and those whose termini fell within a sphere of radius $\delta r = 0.5\langle r^2 \rangle^{1/2}$ around the origin were used to compute the average of $P_1(\gamma)_{r<\delta r} \approx P_1(\gamma)_{r=0}$. Also, following Naghizadeh and Sotobayashi,[22] a single chain of 20 000 monomer units was generated and tested for compliance with the distance requirement, $r_{ij} < \delta r = 0.5\langle r^2 \rangle^{1/2}$, at every monomer unit. The numbers of chains (for the first method) or chain sequences (for the second method) fulfilling the distance requirement are small due to the fact that $W(\mathbf{0})$ is very small for short chains. Hence, the method is inaccurate. The results, not included here, are in approximate agreement, however, with those obtained above by application of eq 1-27.

Corresponding calculations of the averaged Legendre polynomial of second order, $\langle P_2 \rangle_{r=0}$, are plotted against x in Figure 4. Equation 1-27 was truncated at the term $f_{2;2s}$ of the rank $2s$ indicated for the respective sets of data. The points and the lines drawn through them represent results of Monte Carlo calculations for 25 000 chains of each length x. Exact values for $\langle r^2 \rangle$ were substituted in eq 1-23 and the truncated polynomial in eq 1-27 was averaged as a whole. The Hermite series $\mathcal{H}(0)$, truncated at g_4, was used as above. Error bars indicate $2\sigma_m$ limits.

For $x \geq 10$, all $f_{2;2s}$ vanish within indicated limits of error; hence, $\langle P_2 \rangle_{r=0} \approx 0$. Although truncation of eq 1-27 at $f_{2;6}$ obviously is premature for $x < 10$, it is nevertheless noteworthy that $\langle P_2 \rangle_{r=0}$ for $x > 6$ becomes increasingly negative as higher terms are added, whereas for $x = 4$ it becomes steadily more positive as the series is extended.[23] Also, the values obtained for $\langle P_2 \rangle_{r=0}$ are of comparable magnitude to those of $\langle P_1 \rangle_{r=0}$ in this range.

Averaged Legendre polynomials $\langle P_k \rangle_{r=0}$ with $k = 3$–7 were calculated similarly. The results, not included here, demonstrate that terms up to and including $f_{k;6}$ suffice when $x > 10$. The polynomial of third order, $\langle P_3 \rangle_{r=0}$, is zero within its error limits for $x \geq 12$ and positive but very small at $x = 10$ and 11 (ca. 0.02 at $x = 10$ and ca. 0.01 at $x = 11$). All terms of higher

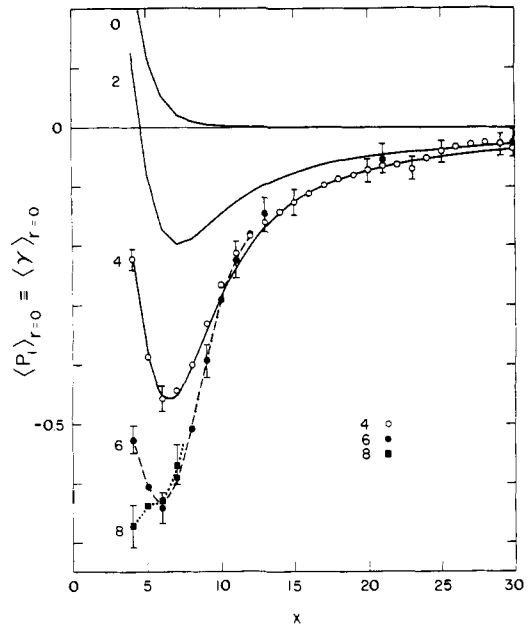

Figure 3. The averaged Legendre polynomial of first order, $\langle P_1\rangle_{r=0}$, calculated according to eq 1-27 truncated at the term $f_{1;2s}$ of the indicated rank $2s$. Solid curves represent exact calculations for $2s = 0$, 2, and 4. Points show results of Monte Carlo calculations. Error bars denote twice the standard error, i.e., $2\sigma_m$.

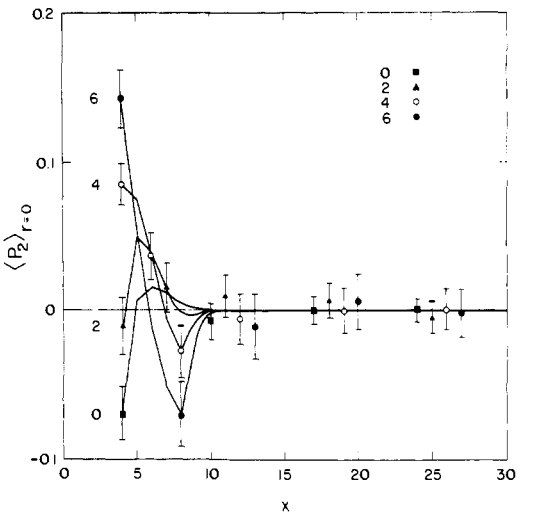

Figure 4. Averaged Legendre polynomial of second order, $\langle P_2\rangle_{r=0}$, calculated according to eq 1-27 truncated at the term $f_{2;2s}$ of the indicated rank $2s$. Points are results from Monte Carlo calculations; error bars show $2\sigma_m$ limits.

order are indistinguishable from zero within limits of accuracy for samples consisting of 25 000 chains at each x. In the range $4 \leq x < 10$, where terms up to and including $f_{k;6}$ do not suffice to define $\langle P_k\rangle_{r=0}$ adequately, $\langle P_3\rangle_{r=0}$ shows a persistent trend toward positive values. Truncation of eq 1-27 at $f_{3;6}$ yields values as large as $\langle P_2\rangle_{r=0}$ for $x = 4$ and 5 (see Figure 4).[23] The polynomials of higher order do not fit a simple pattern. They are negligible for $x > 10$. For small x, most of them assume relatively large positive values, however.

Conditional probability densities $2\Gamma_0(1)$, at $\gamma = 1$ when $\mathbf{r} = \mathbf{0}$, evaluated according to eq 1-19 from the averaged Legendre polynomials $\langle P_k\rangle_{r=0}$ determined above, are presented in Figure 5. The solid curve shows $2\Gamma_0(1)$ obtained by truncation of eq 1-19 at $k = 1$ and eq 1-27 at $f_{1;4}$, the values for $\langle P_1\rangle_{r=0}$ given by the curve labeled "4" in Figure 3 being used. The crosses approximated by the dashed curve were obtained from eq 1-19 terminated at $k = 3$. The additional averaged Legendre polynomials with $k = 2$ and 3 were provided by the Monte Carlo calculations discussed above.

The directional correlation between bonds 1 and $n + 1$ are unfavorable for the formation of rings if $x \geq 10$. The correlation factor $2\Gamma_0(1)$ increases steadily with x but remains appreciably below unity throughout the range of Figure 5. Extension of the calculations to $x = 50$ yields $2\Gamma_0(1) = 0.95$. The calculations, being indecisive for $x < 10$, do not admit of quantitative deductions in this range. However, the tendency of the averaged Legendre polynomials for $k = 1$, 2, and 3 to assume positive and relatively large values for $x = 4$–6 indicates that $2\Gamma_0(1)$ may exceed unity for these small rings.

The lower curve in Figure 5 shows the directional correlation index D_x calculated according to eq 1-30 from the persistence vector $\mathbf{a}$ and the second moment tensor $\langle\rho\rho^T\rangle$ as discussed in 1. This index duplicates the trend of $2\Gamma_0(1)$ with decrease in x but not its magnitude.

The Cyclization Equilibrium Constant K_x

In Figure 6 we compare K_x calculated in various approximations with experimental points over the range $7 \leq x \leq 30$. The spherical Gaussian approximation is shown by the long-dashed curve, which duplicates the uppermost curve in Figure

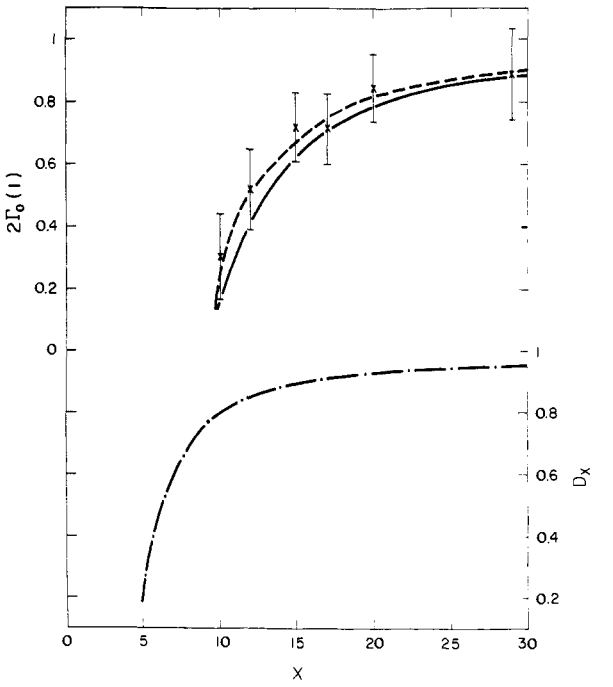

Figure 5. Conditional probability density $\Gamma_0(1)$ of $\gamma \equiv \cos\Delta\theta$ for $\mathbf{r} = \mathbf{0}$ at $\gamma = 1$, multiplied by two and plotted against x. The solid line was obtained from eq 1-19 terminated at $k = 1$ using values of $\langle P_1\rangle_{r=0}$ given by solid curve 4 in Figure 3. Crosses with error bars and the dashed line represent eq 1-19 continued to $k = 3$, the polynomials with $k = 2$ and 3 being evaluated by Monte Carlo methods. The lower curve shows the directional correlation index D_x; see eq 1-30.

2. The dash-dot curve was obtained from eq 1-11, using $W(\mathbf{0})$ given by the scalar Hermite series expansion truncated at g_4, directional correlations between bonds 1 and $n + 1$ being ignored. Over the range covered, this curve differs imperceptibly from curve 4 in Figure 2, calculated using the tensor moment expansion. The solid line represents K_x calculated according to eq 1-14, using $2\Gamma_0(1)$ as given by the solid curve in Figure 5 (estimated from eq 1-19 truncated at $k = 1$; see above). The crosses and the short-dashed curve approximating them are similarly obtained from the points in Figure 5, i.e., they rest on Monte Carlo values of $\langle P_2\rangle_{r=0}$ and $\langle P_3\rangle_{r=0}$, in addition to $\langle P_1\rangle_{r=0}$. Experimental results for the undiluted melt at 110 °C are shown by filled[5] and open[6] circles and for solutions in

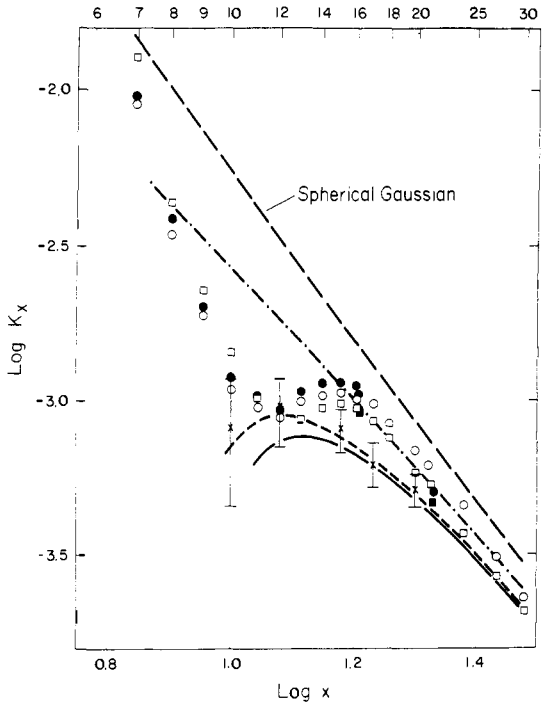

Figure 6. Cyclization equilibrium constant K_x vs. x. The long-dashed line represents the Gaussian approximation, the dot-dashed line represents K_x calculated according to eq 1-11 from $W(\mathbf{0})$ as given by the scalar Hermite series expansion truncated at g_4, directional correlations between chain ends being neglected. The solid line was obtained according to eq 1-14 with $2\Gamma_0(1)$ taken from the solid line in Figure 5. The dashed curve, crosses, and $2\sigma_m$ error bars were obtained from the Monte Carlo calculations, represented in like manner as in Figure 5. Experimental points: (○) bulk at 110 °C, Semlyen and Wright;[5] (●) bulk at 110 °C, Wright;[6] (■) toluene at 108 °C, Wright;[6] (□) toluene at 110 °C, taken from the curve of Brown and Slusarczuk.[3]

toluene at a concentration of 23 g $l.^{-1}$ at 55 °C by open[3] and filled squares.[6] Results obtained in diglyme[6] at the same concentration and temperature are indistinguishable from those in toluene over the range of x shown in Figure 6.

Whereas the calculations yield values of the direction correlation factor $2\Gamma_0(1)$ that depart appreciably from unity as x falls below 30 units, the experimental results are in excellent agreement with the curve (dash-dot) calculated neglecting angle correlations for all $x > 15$, as was pointed out above. Thus, agreement with the experimental results is worsened for $x = 15$–30 by inclusion of the directional correlation factor. A maximum is indicated in the theoretical curves that include the angle correlation, and the calculations of $\langle P_k \rangle_{r=0}$ offer evidence of a probable minimum at a small value of x. These features are displaced considerably from the observed maximum and minimum, however. In fact, the calculated maximum appears to occur in the vicinity of the experimental minimum in K_x at $x = 12$. The coincidence of calculated and experimental values at this point must be regarded as coincidental.[26]

On the other hand, the theoretical calculations give values of $2\Gamma_0(1)$ that are smaller than unity and are approximately of the magnitude indicated by the experimental data. Even in the range $x = 15$–18 where the divergence between theory and experiment is greatest, the differences are scarcely greater than the combined errors in the experimental data (5 to 10%) and in the calculations as indicated by the error bars.

Acknowledgment. This work was supported by the National Science Foundation, Grant No. DMR-73-07655 A02. One of the authors (M.M.) is grateful to the Deutsche Forschungsgemeinschaft for the award of a fellowship.

Appendix. Generator Matrices for $\langle \gamma^m r^{2p} \rangle$

The quantities required for the calculation of $\langle P_k \rangle_{r=0}$ by series expansion according to eq 1-22 and 1-23 are $\langle \gamma^m r^{2p} \rangle$ with $m \geq 0$ and $p \geq 0$. Applying the general method[19] for calculation of a constitutive property of a chain of n bonds in a specified conformation, we have for any positive power of the magnitude of the chain vector

$$r^{2p} = \mathbf{G}_{[1}^{\times p}(\mathbf{G}^{\times p})_2^{(n-2)}\mathbf{G}_{n]}^{\times p} \tag{A1}$$

where the superscript $\times p$ denotes the self-direct product of the generator matrix $\mathbf{G}$ for the bond denoted by subscript, and $(\mathbf{G}^{\times p})_2^{(n-2)}$ represents the serial product of $n - 2$ of these self-direct products commencing with $(G^{\times p})_2$. The generator matrix $\mathbf{G}_i$ for r^2 is given by

$$\mathbf{G}_i = \begin{bmatrix} 1 & 2\mathbf{1}^T\mathbf{T} & l^2 \\ 0 & \mathbf{T} & \mathbf{1} \\ 0 & \mathbf{0} & 1 \end{bmatrix}, \quad 1 < i < n \tag{A2}$$

where $\mathbf{T}_i$ is the matrix of the transformation from the reference frame of bone $i + 1$ to that of bond i[10,19] The matrix $\mathbf{G}_{[1}$ for the first bond is given by the first row of $\mathbf{G}_1$; the matrix $\mathbf{G}_{n]}$ for the nth bond is given by the last column of $\mathbf{G}_n$. The square order of $\mathbf{G}^{\times p}$ can be reduced from $5p$ by combining redundant elements[24,25] to (p_p^+4). Thus $\mathbf{G}^{\times 3}$ can be reduced from order 125×125 to 35×35.

The cosine of the angle $\Delta\theta$ between bonds 1 and $n + 1$ is given by

$$\gamma = [100]\mathbf{T}_1^{(n)}\begin{bmatrix}1\\0\\0\end{bmatrix} \tag{A3}$$

By use of the identity $\gamma^m \equiv \gamma^{\times m}$ we obtain

$$\gamma^m = [100]^{\times m}(\mathbf{T}^{\times m})_{1(n)}\begin{bmatrix}1\\0\\0\end{bmatrix}^{\times m} \tag{A4}$$

Again, the square order of the self-direct products of $\mathbf{T}$ can be reduced to $(m \overset{+}{m} 2)$.[24]

The product $\gamma^m r^{2p}$ of these scalar quantities for the chain of n bonds and an additional hypothetical bond $n + 1$ is given by

$$\gamma^m r^{2p} = \{([100]\mathbf{T}_1)^{\times m} \otimes G_{[1}^{\times p}\} \times \mathbf{Y}_2^{(n-1)}\left\{\begin{bmatrix}1\\0\\0\end{bmatrix}^{\times m} \otimes \begin{bmatrix}0\\0\\0\\0\\1\end{bmatrix}^{\times p}\right\} \tag{A5}$$

where

$$\mathbf{Y}_i = (\mathbf{T}^{\times m} \otimes \mathbf{G}^{\times p})_i \tag{A6}$$

The column matrix col(0,0,0,0,1) is required since r^{2p} is measured for the chain with n bonds only while γ stands for the relative orientation of bonds 1 and $n + 1$; col(0,0,0,0,1) represents $\mathbf{G}_{n+1]}$ for a bond of zero length. The order of $\mathbf{Y}_i$ can be diminished by using the reduced self-direct products mentioned above. The generator matrix for $\gamma^2 r^2$, for instance, is condensed from 225×225 to 90×90 order.

The required configurational average is given by[19]

$$\langle \gamma^m r^{2p} \rangle = Z^{-1}\mathcal{Y}_{[1}\mathcal{Y}_2^{(n-2)}\mathcal{Y}_{n]} \tag{A7}$$

where Z is the configuration partition function given by the

serial product $\mathbf{U}_1^{(n)}$ of statistical weight matrices $\mathbf{U}_i$ (see eq 1), and

$$\mathcal{Y}_i = (\mathbf{U}_i \otimes \mathbf{E}_t)\|\mathbf{Y}_i\|, \quad 1 < i < n \tag{A8}$$

$\|\mathbf{Y}_i\|$ is the diagonal array of the generator matrices $\mathbf{Y}_i$ for the several rotational states for bond i, and $\mathbf{E}_t$ is the unit matrix of the same order t as $\mathbf{Y}_i$. The terminal matrices in eq A7 are given by[19,20]

$$\mathcal{Y}_{[1} = \mathbf{U}_1 \otimes \mathbf{Y}_{[1}$$
$$\mathcal{Y}_{n]} = \mathbf{U}_n \otimes \mathbf{Y}_{n]} \tag{A9}$$

References and Notes

(1) J. A. Semlyen, review, in press.
(2) D. W. Scott, *J. Am. Chem. Soc.*, **68**, 2294 (1946).
(3) J. F. Brown, Jr., and G. M. J. Slusarczuk, *J. Am. Chem. Soc.*, **87**, 931 (1965).
(4) J. B. Carmichael and R. Winger, *J. Polym. Sci., Part A*, **3**, 971 (1965).
(5) J. A. Semlyen and P. V. Wright, *Polymer*, **10**, 543 (1969); P. V. Wright and J. A. Semlyen, *ibid.*, **11**, 462 (1970).
(6) P. V. Wright, *J. Polym. Sci., Polym. Phys. Ed.*, **11**, 51 (1973).
(7) P. J. Flory, U. W. Suter, and M. Mutter, *J. Am. Chem. Soc.*, part 1 in this issue.
(8) M. S. Beevers and J. A. Semlyen, *Polymer*, **13**, 385 (1972).
(9) J. A. Semlyen and P. J. Flory, *J. Am. Chem. Soc.*, **88**, 3209 (1966).
(10) P. J. Flory, "Statistical Mechanics of Chain Molecules", Interscience, New York, N.Y., 1969; see especially pp 392-396.
(11) H. Jacobson and W. H. Stockmayer, *J. Chem. Phys.*, **18**, 1600 (1950).
(12) J. E. Mark and P. J. Flory, *J. Am. Chem. Soc.*, **86**, 138 (1964).
(13) P. J. Flory, V. Crescenzi, and J. E. Mark, *J. Am. Chem. Soc.*, **86**, 146 (1964).
(14) P. J. Flory, *Proc. Natl. Acad. Sci. U.S.A.*, **70**, 1819 (1973).
(15) D. Y. Yoon and P. J. Flory, *J. Chem. Phys.*, **61**, 5366 (1974).
(16) P. J. Flory and V. W. C. Chang, *Macromolecules*, **9**, 33 (1976).
(17) V. W. C. Chang, Ph.D. Thesis, Stanford University, 1975.
(18) Reference 10, pp 174-180.
(19) P. J. Flory, *Macromolecules*, **7**, 381 (1974).
(20) P. J. Flory and D. Y. Yoon, *J. Chem. Phys.*, **61**, 5358 (1974).
(21) M. Mutter, U. W. Suter, and P. J. Flory, *J. Am. Chem. Soc.*, part 3 in this issue.
(22) J. Naghizadeh and H. Sotobayashi, *J. Chem. Phys.*, **60**, 3104 (1974).
(23) The RIS scheme applicable to longer sequences breaks down for cyclization of the tetramer owing to the fact that coalescence of the terminal Si atoms, and appended groups, in the hypothetical process of cyclization (see Figure 1) eliminates the second-order interaction responsible for $\omega = 0$ in eq 1. The same circumstance occurs in the closure of the six-membered polymethylene sequence. This qualification of the treatment, which does not apply to larger rings, has been noted and taken into account by Semlyen and Wright[5] and by M. Sisido, *Macromolecules*, **4**, 737 (1971). Calculations in the text for $x = 4$ are for illustration only and are not applicable to actual tetrameric rings.
(24) K. Nagai, *J. Chem. Phys.*, **48**, 5646 (1968); K. Nagai, *ibid.*, **38**, 924 (1963); K. Nagai and T. Ishikawa, *ibid.*, **45**, 3128 (1966).
(25) P. J. Flory and Y. Abe, *J. Chem. Phys.*, **47**, 1999 (1967).
(26) NOTE ADDED IN PROOF. L. E. Scales and J. A. Semlyen, *Polymer*, **17**, 601 (1976), attribute the minimum and maximum in K_x for $x = 10$-13 to peculiarities of the PDMS conformations arising from the inequality of the bond angles at O and Si. By enumeration of all conformations, they find that, within this range of x, the probability $W(\mathbf{0})$ depends critically on the precise value assigned to the bond angle at O. The locations of the extrema in K_x are considered therefore to be related to this structural feature of the PDMS chain.

Macrocyclization Equilibria. 3. Poly(6-aminocaproamide)

M. Mutter, U. W. Suter, and P. J. Flory*

Contribution from the Department of Chemistry, Stanford University, Stanford, California 94305.

Received March 3, 1976

Abstract: The probability density function $W(\mathbf{0})$ at $r = \mathbf{0}$ and the directional correlation factors $2\Gamma_0(1)$ for homologous poly(6-aminocaproamide) sequences with $x = 2$ to 7 units (14-49 bonds) are evaluated and the influences of these factors on the cyclization equilibria constants K_x are determined through application of the theory presented in the first paper of this series. For $x = 3$-6, the departure of $W(\mathbf{0})$ from its value for the Gaussian distribution accounts for ca. 60% of the discrepancies between experimental results and calculations according to the theory of Jacobson and Stockmayer. The inclusion of the factor for orientational correlations between terminal bonds further depresses K_x by ca. 60% for $x = 3$, 30% for $x = 4$, and 20-25% for $x = 5$ and 6. Agreement of theory with published experimental results for $x = 3$-6 is within limits set by uncertainties in the calculations combined with the experimental errors, i.e., within about 15%.

Poly(6-aminocaproamide), (PACA), normally synthesized by polymerization of ϵ-caprolactam, contains cyclic species $[NH(CH_2)_5CO]_x$ in the amount of ca. 12% in the melt at 500 to 550 K at equilibrium with the linear polymer.[1,2] Of this, ca. 3-4% comprises cyclic oligomers for which $x \geq 2$. The cyclization constants K_x for x-meric rings with $x = 1$-6 have been determined by Semlyen and co-workers[1] and earlier by Zahn, Rothe, and their co-workers.[2] Gas-liquid chromatography was used in these experiments for determination of the concentrations of cyclic monomer and dimer; gel permeation chromatography was employed for $x = 3$-6, and it was applied as an alternative method for $x = 1$ and 2. Inasmuch as the repeat unit comprises seven members, successive oligomers are more easily separated than members of the PDMS series[3] discussed in the preceding paper,[4] designated 2. Hence, the results for PACA should be less subject to errors of analysis.

In keeping with observations on most of the other series of cyclic homologues that have been investigated,[3,5-7] the experimental cyclization constants for PACA[1,2] in the intermediate range $x = 2$-6 are substantially smaller than values calculated according to the theory of Jacobson and Stockmayer[8] under the assumption that the density of chain vectors $\mathbf{r}$ at $\mathbf{r} = \mathbf{0}$ is given by the spherical Gaussian distribution; see eq 12 of the first paper[9] of this series, hereafter designated as 1. The rotational isomeric state analysis of the configurational statistics of linear PACA chains carried out by Williams and one of the present authors[10] provides the basis for calculation of the second moment $\langle r_x^2 \rangle$ required for evaluation of the Gaussian density. The values of K_x for PACA show even greater departures from theory (eq 1-12) based on the Gaussian density than has been observed in other systems. Thus, the ratios of observed values of K_2, K_3, K_4, K_5, and K_6 to those calculated in this manner are 0.17, 0.26, 0.48, 0.53, and 0.45, respectively.

In this paper we apply the treatment set forth in 1[9] and applied to PDMS in 2[4] to the PACA chain having a repeat unit that embraces a greater variety of skeletal bonds, including the